CEAS-GNC-2022-071

CEAS EuroGNC 2022
"Conference on Guidance, Navigation and Control"
3-5 May 2022 @ Technische Universität Berlin, Germany

Guidance of Gliding Vehicles with Energy Management Based on Approximate Prediction of Speed

Namhoon Cho Research Fellow, Centre for Autonomous and Cyber-Physical Systems, School of Aerospace, Transport and Manufacturing, Cranfield University, MK43 0AL, Cranfield, Bedfordshire, United Kingdom. n.cho@cranfield.ac.uk

Youngil Kim PhD Student, Department of Aerospace Engineering, Seoul National University, 08826, Seoul, Republic of Korea. calav3@snu.ac.kr

Hyo-Sang Shin Professor of Guidance, Control, and Navigation Systems, Centre for Autonomous and Cyber-Physical Systems, School of Aerospace, Transport and Manufacturing, Cranfield University, MK43 0AL, Cranfield, Bedfordshire, United Kingdom. h.shin@cranfield.ac.uk

Youdan Kim Professor, Department of Aerospace Engineering, Institute of Advanced Aerospace Technology, Seoul National University, 08826, Seoul, Republic of Korea. ydkim@snu.ac.kr

ABSTRACT

This study presents a guidance method for flight vehicles gliding in the vertical plane to achieve desired position and velocity at the final time. The proposed guidance algorithm combines two decoupled elements to plan future flight trajectories satisfying the given constraints at each guidance update cycle: i) parametric path generator, and ii) approximate speed predictor. The parametric path generator is capable of producing an altitude profile as a parametric function of downrange by solving a convex optimisation problem considering only the shape properties of a flight path. An approximate method for predicting the future speed history endows the proposed guidance algorithm with the capability to address energy management objectives in trajectory planning. Provided that an altitude profile is specified by the parametric path generator and the lift-to-drag ratio model is known, the approximation neglecting gravitational acceleration turns the speed dynamics along the given path into a scalar linear first order ordinary differential equation, the form which admits a closed-form solution that can be represented by definite integrals. In this way, the proposed method opens a possibility to update the trajectory in flight to achieve the desired final speed by reducing the computational load due to speed prediction task, although the predicted speed contains approximation errors of certain degrees.

Keywords: Speed Prediction; Energy Management; Guidance; Glide Vehicles

1 Introduction

The necessity to dissipate a specific amount of the mechanical energy during flight poses a significant challenge to the trajectory planning and guidance of endoatmopheric gliding vehicles. The difficulty arises mainly from the absence of an active control effector over the speed of vehicle such as an engine that provides thrust or a speed brake that yields additional drag. With the general understanding about

the vehicle aerodynamics that both drag and lift increase in magnitude with increasing angle-of-attack unless flow separation does not take place, the only available way to cope with the problem of energy management is to perform lateral manoeuvres intended for producing certain amount of drag. For this reason, a trajectory should be designed by explicitly considering the speed variation while meeting all the other constraints including the desired position and flight path angle at the final time. However, another major difficulty lies in the prediction of speed in that the differential equation for vehicle speed directly depends on the drag model and its solution can be obtained by relying on numerical integration which may demand a substantial amount of computational load. As a consequence, trajectory planning to achieve a desired mechanical energy in addition to the usual position and arrival direction conditions at the end of flight has remained a difficult task to be performed online.

Trajectory planning and/or guidance to achieve a desired final speed in arrival-angle-constrained missions have attracted relatively less attention in comparison to the problem of maximising the final speed. The notion of minimising the control effort defined by the amount of lateral acceleration to keep the induced drag small applies well only to the final speed maximisation problem. The approaches developed for energy management guidance with arrival direction constraint include the method based on stitched path primitives and drag reference tracking [1–3], the impact-angle-control guidance law including a term providing explicit feedback over the predicted final speed error [4], the method of finding a tuning coefficient in an impact-angle-control guidance law that results in a trajectory meeting the desired final speed [5], and the simulation-based framework for pre-planning of waypoints [6]. The Terminal Area Energy Management (TAEM) guidance method described in [1] for the approach and landing phase of the space shuttle takes several heuristic choices in its design by using circular or spiral-like horizontal path for dumping excessive energy. It might not be applicable in an identical manner to other types of gliding vehicles that is confined to fly in the vertical plane. The approach involving a mathematical expression for the lateral acceleration command rather than an algorithmic description is quite intuitive and reliable. However, the guidance law presented in [4, 5] relies on brute-force numerical propagation of the entire set of differential equations describing motion under a baseline guidance law. The speed prediction method presented in [7] obtains the estimate in closed form, however, it is inappropriate for vehicles performing manoeuvres in the vertical plane since it assumes constant flight path angle for the steady glide condition and a specific drag-lift relationship. The waypoint planning framework of [6] enables systematic design of mission considering the dynamic feasibility of planning solution, but the large computational burden due to repeated simulation limits its application in an online setting.

The main objective of this study is to develop a computationally efficient guidance algorithm for generating manoeuvres in the vertical plane to achieve desired position and velocity at the final time. The previous studies suggest that an energy management trajectory planning algorithm inevitably requires a speed predictor in some form and speed prediction is the most time-consuming step in the planning pipeline. Iterative targetting of the desired final speed with the predicted trajectory is also necessary at each planning update cycle to find the solution among many trajectories satisfying all the constraints imposed on the geometric properties of the flight path at the initial and final points. Motivated by these observations, the present study pursues a direction that can reduce the amount of computation needed in speed prediction. To this end, the proposed guidance algorithm combines i) a path generator that can produce one-parameter family of curves interpolating given boundary conditions in the form of downrange-referenced altitude profiles and ii) an approximate speed predictor that yields a semi-analytical solution for the single differential equation describing speed variation with respect to downrange. The approximation that neglects gravity in the process of relating the lift coefficient with the curvature of given path is the key that reduces the number of equations involved, thus leading to the improvement in computational efficiency at the cost of losing accuracy.

The rest of the paper is organised as follows: Section 2 describes the equation of motion and the guidance problem considered in this study. Section 3 presents the guidance algorithm with detailed description of the path generator and the approximate speed predictor. In Sec. 4, simulation examples

demonstrate the performance of the proposed algorithm, and Sec. 5 concludes the paper with summarising remarks.

2 Problem Formulation

2.1 Equation of Motion

This study considers an unpowered gliding vehicle that flies inside the atmosphere and assumes that the vehicle can be modelled as a point mass moving on the vertical plane that perfectly achieves the commanded lift acceleration. The equations of motion with time t as the independent variable can be expressed as

$$\dot{x} = V\cos\gamma \tag{1}$$

$$\dot{h} = V\sin\gamma \tag{2}$$

$$\dot{\gamma} = \frac{L}{mV} - \frac{g}{V}\cos\gamma \tag{3}$$

$$\dot{V} = -\frac{D}{m} - g\sin\gamma \tag{4}$$

where $(\dot{\cdot}) = \frac{d}{dt}()$, and x, h, γ, and V denote the downrange, the altitude, the flight path angle, and the speed, respectively. Also, m and g represent the dry mass and the gravitational acceleration, respectively, and L and D are the lift and the drag defined as

$$L = \frac{1}{2}\rho V^2 S C_L \tag{5}$$

$$D = \frac{1}{2}\rho V^2 S C_D \tag{6}$$

with ρ, S, C_L, and C_D referring to the atmospheric density, the reference area, the lift coefficient, and the drag coefficient, respectively. Note that m, g, and S are constants, and ρ is generally a function of h. The aerodynamic coefficients C_L and C_D are functions of the angle-of-attack α and the Mach number, in general.

Assuming that x increases monotonically with respect to t, i.e., $\gamma \in \left(-\frac{\pi}{2}, \frac{\pi}{2}\right)$, the independent variable of the differential equations can be changed from t to x by dividing Eqs. (2)-(4) with Eq. (1) as follows:

$$h' = \tan\gamma \tag{7}$$

$$\gamma' = \frac{L}{mV^2\cos\gamma} - \frac{g}{V^2} \tag{8}$$

$$V' = -\frac{D}{mV\cos\gamma} - \frac{g}{V}\tan\gamma \tag{9}$$

where $(\cdot)' = \frac{d}{dx}$.

2.2 Trajectory Planning Problem

The desired final position as well as the desired final flight path angle are usually considered to have certain fixed values that meet the mission requirements. Provided that the final altitude is specified, demanding a particular level of mechanical energy for the final time is equivalent to achieving a desired final speed. Also, Eq. (7) indicates that the downrange-derivative of the altitude can be related to the flight path angle. The trajectory planning problem considered in this study is to find a spatial curve $h(x)$

that satisfies the boundary conditions given by

$$h(x_t) = h_t \qquad h(x_f) = h_{f_d} \tag{10}$$

$$h'(x_t) = \tan\gamma_t \qquad h'(x_f) = \tan\gamma_{f_d} \tag{11}$$

$$V(x_f) = V_{f_d} \tag{12}$$

where the subscript notation $(\cdot)_t$ and $(\cdot)_{f_d}$ represent the current and the desired final value of a quantity, respectively. Note that the requirement $h''(x_f) = -\frac{g}{\left(V_{f_d}\cos\gamma_{f_d}\right)^2}$ can be included explicitly to the set of boundary conditions if nullification of terminal lift acceleration is necessary to avoid large manoeuvres at the end of flight so that the vehicle has enough aerodynamic control authority to deal with uncertainties.

3 Guidance Algorithm

3.1 Relation Between Path Geometry and Vehicle Motion

Suppose that the flight path is given as an altitude profiled $h(x)$. It is obvious from Eq. (7) that the corresponding flight path angle profile can be obtained as

$$\gamma(x) = \tan^{-1}\left(h'(x)\right) \tag{13}$$

Differentiating Eq. (13) with respect to x yields

$$\gamma'(x) = \frac{h''(x)}{1+\{h'(x)\}^2} = h''(x)\cos^2\gamma(x) \tag{14}$$

By equating the relation for path geometry in Eq. (14) with the expression for vehicle motion in Eq. (8), the corresponding lift acceleration profile can be represented as

$$A_L(x) = \frac{L}{m} = \left\{h''(x)\cos^2\gamma(x)\{V(x)\}^2 + g\right\}\cos\gamma(x) \tag{15}$$

with $\gamma(x)$ given in Eq. (13). Evaluating Eq. (15) at the current point x_t by using the value of $h''(x_t)$ obtained from the planned trajectory and the measurements (or estimates) for h, γ, and V gives the lift acceleration command at each instance which can be supplied as the reference to a normal acceleration autopilot.

3.2 Parametric Path Generation

The trajectory that satisfies the path geometry boundary conditions given by Eqs. (10) and (11) is not unique. Additional free parameters available for trajectory shaping can be exploited to generate multiple feasible trajectories having different final speeds. In this respect, one possible approach based on the concept known as iterative targetting is to find one trajectory satisfying the final speed boundary condition given by Eq. (12) through iterative correction of the trajectory shaping parameter. Having only a single degree-of-freedom for tuning is preferable for better computational efficiency and reliability of the iterative solution process. Therefore, a path generator needs to be capable of producing a wide enough range of candidate trajectories by tuning of a single trajectory shaping parameter.

For this purpose, this study employs a simple convex optimisation approach based on Quadratic Programming (QP) to generate the path as a parametric curve satisfying the position and the tangent boundary conditions at the end points. Let us first consider the normalisation of variables for enhanced stability and efficiency of numerical solution process. The normalised downrange and altitude are defined

by

$$\bar{x} \triangleq \frac{x}{x_{ref}} \tag{16}$$

$$\bar{h} \triangleq \frac{h}{h_{ref}} \tag{17}$$

where x_{ref} and h_{ref} are the characteristic downrange and altitude chosen to make both $\bar{x}$ and $\bar{h}$ lie in a similar range. Let $(\cdot)^{\circ} \triangleq \frac{d}{d\bar{x}}$ denote the differentiation with respect to $\bar{x}$. Using the relation $\bar{h}^{\circ} = \frac{x_{ref}}{h_{ref}} h'$, the boundary conditions in Eqs. (10) and (11) can be rewritten in terms of the normalised variables as

$$\bar{h}\left(\bar{x}_t\right) = \bar{h}_t \qquad \bar{h}\left(\bar{x}_f\right) = \bar{h}_{f_d} \tag{18}$$

$$\bar{h}^{\circ}\left(\bar{x}_t\right) = \frac{x_{ref}}{h_{ref}} \tan\gamma_t \qquad \bar{h}^{\circ}\left(\bar{x}_f\right) = \frac{x_{ref}}{h_{ref}} \tan\gamma_{f_d} \tag{19}$$

where $\bar{x}_t = \frac{x_t}{x_{ref}}$, $\bar{x}_f = \frac{x_f}{x_{ref}}$, $\bar{h}_t = \frac{h_t}{h_{ref}}$, and $\bar{h}_{f_d} = \frac{h_{f_d}}{h_{ref}}$.

Consider a linearly-parametrised form for the path that represents $\bar{h}$ as a function of $\bar{x}$ as

$$\bar{h}\left(\bar{x}\right) = \boldsymbol{\phi}^T\left(\bar{x}\right)\mathbf{c} \tag{20}$$

where $\boldsymbol{\phi}\left(\bar{x}\right) : \mathbb{R} \mapsto \mathbb{R}^{p\times 1}$ is the basis function vector, and $\mathbf{c} \in \mathbb{R}^{p\times 1}$ is the coefficient vector. The number of undetermined coefficients should be no less than the number of boundary conditions for existence of a solution, therefore, the dimension should be chosen to satisfy $p \geq 4$ in the present study. The type of basis functions determines the overall behavioural characteristics of the curve, hence, its choice is indeed a design parameter for trajectory shaping. However, more flexibility can be provided instead by overparametrising the curve yet using a standard basis function such as polynomials. That is, taking $p > 4$ will allow more degrees-of-freedom for systematic curve design. In this underdetermined case, the coefficient vector can be fully determined by solving a QP problem formulated for path design under constraints with the coefficients as the decision variable. One special problem that is useful for the purpose of energy management in the vertical plane is to minimise a performance index given by

$$J\left(R\right) = \int_{\bar{x}_t}^{\bar{x}_f} \left[\left\{\bar{h}\left(s\right) - \bar{h}_{des}\right\}^2 + 10^R \left\{\bar{h}^{\circ\circ}\left(s\right)\right\}^2\right] ds \tag{21}$$

which measures the weighted sum of the path curvature and the gap between the path and a constant desired altitude $\bar{h}_{des} = \frac{h_{des}}{h_{ref}}$ with the constant weight R that can either be negative or positive, subject to the boundary conditions, Eqs. (18) and (19). By introducing the parametric structure shown in Eq. (20), the optimisation problem can be represented as the following QP problem with the coefficient vector $\mathbf{c}$ as the optimisation variable

$$\begin{aligned} &\text{minimise} \quad J\left(R\right) = \mathbf{c}^T\mathbf{P}\mathbf{c} + \mathbf{q}^T\mathbf{c} \\ &\text{subject to} \quad \mathbf{A}\mathbf{c} = \mathbf{b} \end{aligned} \tag{22}$$

In Eq. (22), the problem data matrices are given by

$$\mathbf{P} = \int_{\bar{x}_t}^{\bar{x}_f} \left\{\boldsymbol{\phi}\left(s\right)\boldsymbol{\phi}^T\left(s\right) + 10^R \boldsymbol{\phi}^{\circ\circ}\left(s\right)\boldsymbol{\phi}^{\circ\circ T}\left(s\right)\right\} ds, \quad \mathbf{q} = -2\bar{h}_{des}\int_{\bar{x}_t}^{\bar{x}_f} \boldsymbol{\phi}\left(s\right) ds$$

$$\mathbf{A} = \begin{bmatrix} \boldsymbol{\phi}^T\left(\bar{x}_t\right) \\ \boldsymbol{\phi}^T\left(\bar{x}_f\right) \\ \boldsymbol{\phi}^{\circ T}\left(\bar{x}_t\right) \\ \boldsymbol{\phi}^{\circ T}\left(\bar{x}_f\right) \end{bmatrix}, \qquad \mathbf{b} = \begin{bmatrix} \bar{h}_t \\ \bar{h}_{f_d} \\ \frac{x_{ref}}{h_{ref}}\tan\gamma_t \\ \frac{x_{ref}}{h_{ref}}\tan\gamma_{f_d} \end{bmatrix} \tag{23}$$

For the particular choice of the basis function vector given by $\boldsymbol{\phi}(s) = \begin{bmatrix} s^{p-1} & s^{p-2} & \cdots & s & 1 \end{bmatrix}^T$, the integrals in Eq. (23) can be obtained analytically as follows:

$$\mathbf{S} = \int_{\bar{x}_t}^{\bar{x}_f} \left\{ \boldsymbol{\phi}(s) \boldsymbol{\phi}^T(s) \right\} ds = \begin{bmatrix} \frac{\bar{x}_f^{2p-1} - \bar{x}_t^{2p-1}}{2p-1} & \frac{\bar{x}_f^{2p-2} - \bar{x}_t^{2p-2}}{2p-2} & \cdots & \frac{\bar{x}_f^{p+1} - \bar{x}_t^{p+1}}{p+1} & \frac{\bar{x}_f^{p} - \bar{x}_t^{p}}{p} \\ \frac{\bar{x}_f^{2p-2} - \bar{x}_t^{2p-2}}{2p-2} & \frac{\bar{x}_f^{2p-3} - \bar{x}_t^{2p-3}}{2p-3} & \cdots & \frac{\bar{x}_f^{p} - \bar{x}_t^{p}}{p} & \frac{\bar{x}_f^{p-1} - \bar{x}_t^{p-1}}{p-1} \\ \vdots & \vdots & \ddots & \vdots & \vdots \\ \frac{\bar{x}_f^{p+1} - \bar{x}_t^{p+1}}{p+1} & \frac{\bar{x}_f^{p} - \bar{x}_t^{p}}{p} & \cdots & \frac{\bar{x}_f^{3} - \bar{x}_t^{3}}{3} & \frac{\bar{x}_f^{2} - \bar{x}_t^{2}}{2} \\ \frac{\bar{x}_f^{p} - \bar{x}_t^{p}}{p} & \frac{\bar{x}_f^{p-1} - \bar{x}_t^{p-1}}{p-1} & \cdots & \frac{\bar{x}_f^{2} - \bar{x}_t^{2}}{2} & \bar{x}_f - \bar{x}_t \end{bmatrix}$$

$$\text{or } [\mathbf{S}]_{ij} = \frac{\bar{x}_f^{2p-(i+j-1)} - \bar{x}_t^{2p-(i+j-1)}}{2p-(i+j-1)} \tag{24}$$

$$\mathbf{H} = \begin{bmatrix} \mathbf{0}_{(p-2)\times 2} & \operatorname{diag}\left(\begin{bmatrix} (p-1)(p-2) & (p-2)(p-3) & \cdots 2 \end{bmatrix} \right) \\ \mathbf{0}_{2\times 2} & \mathbf{0}_{2\times(p-2)} \end{bmatrix}$$

$$\mathbf{P} = \mathbf{S} + 10^R \mathbf{H}\mathbf{S}\mathbf{H}^T$$

$$\mathbf{q} = -2\bar{h}_{des}\mathbf{S}[:, p]$$

3.3 Approximate Speed Prediction

The parametric path generator described in the previous section provides an altitude profile as $h(x) = h_{ref}\boldsymbol{\phi}^T\left(\frac{x}{x_{ref}}\right)\mathbf{c}^*$ with the optimal coefficient $\mathbf{c}^*$ for each combination of shaping parameters, e.g., R and h_{des}. The first and second derivatives of the altitude profile can be obtained in terms of the derivatives of the basis functions as $h'(x) = \frac{h_{ref}}{x_{ref}}\boldsymbol{\phi}^{\circ T}\left(\frac{x}{x_{ref}}\right)\mathbf{c}^*$ and $h''(x) = \frac{h_{ref}}{x_{ref}^2}\boldsymbol{\phi}^{\circ\circ T}\left(\frac{x}{x_{ref}}\right)\mathbf{c}^*$. The flight path angle profile and its first derivative can be computed according to Eqs. (13) and (14), respectively. Then, by substituting Eq. (5) into Eq. (8), the lift coefficient profile that corresponds to the given trajectory can be expressed as

$$\frac{\rho(h(x))S}{2m\cos\gamma(x)} C_L(x) = \gamma'(x) + \frac{g}{\{V(x)\}^2} \tag{25}$$

However, the speed profile $V(x)$ in Eq. (25) is not available as a pre-specified information since it could only be obtained by solving the associated differential equation. At this point, let us introduce an approximation that the term $\frac{g}{\{V(x)\}^2}$ in Eq. (25) is non-dominant and a rough initial guess for the speed given by $\hat{V}_{guess}(x)$ is only available. Note that one can simply take $\hat{V}_{guess}(x) = \infty$ to completely neglect the effect of gravity term in Eq. (25), or a simple function of downrange satisfying $\hat{V}_{guess}(x_0) = V_0$ and $\hat{V}_{guess}(x_f) = V_{fd}$ can also be used as the initial guess. One such example of the initial guess for the speed profile is given by

$$\hat{V}_{guess}(x) = V_{fd} - (V_{fd} - V_0)\left(\frac{x_f - x}{x_f - x_0}\right)^n \tag{26}$$

where $n > 0$. Also, refinement can be performed by taking the predicted speed solution again as the initial guess for subsequent iteration. This approximation then leads us to

$$\frac{\rho(h(x))S}{2m\cos\gamma(x)} C_L(x) \approx \gamma'(x) + \frac{g}{\left\{\hat{V}_{guess}(x)\right\}^2} \tag{27}$$

Now, by substituting Eq. (6 into Eq. (9), assuming that the drag coefficient has functional dependence on the lift coefficient, and applying the approximation described by Eq. (27), we have

$$\begin{aligned} V'(x) &= -\frac{\rho(h(x))S}{2m\cos\gamma(x)} C_L(x) \frac{C_D(C_L(x))}{C_L(x)} V(x) - \frac{g}{V(x)} \tan\gamma(x) \\ &= -\left\{ \gamma'(x) + \frac{g}{\left\{\hat{V}_{guess}(x)\right\}^2} \right\} C_{D/L}(x) V(x) - \frac{g}{V(x)} \tan\gamma(x) \end{aligned} \tag{28}$$

where $C_{D/L} \triangleq \frac{C_D}{C_L}$ denotes the drag-to-lift ratio which can be regarded as a function of x. Equation (28) can be transformed into a first-order linear ordinary differential equation of the specific kinetic energy $\mathcal{K} \triangleq \frac{1}{2}V^2$ as

$$\begin{aligned} \mathcal{K}'(x) &= -2\left\{ \gamma'(x) + \frac{g}{\left\{\hat{V}_{guess}(x)\right\}^2} \right\} C_{D/L}(x) \mathcal{K}(x) - g\tan\gamma(x) \\ &\triangleq a(x)\mathcal{K}(x) + b(x) \end{aligned} \tag{29}$$

where $a(x)$ and $b(x)$ are the coefficient functions defined accordingly. The solution for the linear dynamics described in Eq. (29) can be obtained analytically. Solving Eq. (29) for the closed interval $[x, x_f]$ gives a closed-form expression for the final specific kinetic energy predicted at each instance x as

$$\hat{\mathcal{K}}(x_f) = \Phi(x_f; x)\mathcal{K}(x) + \int_x^{x_f} \Phi(x_f; s) b(s)\, ds \tag{30}$$

where

$$\Phi(x; s) = \exp\left(\int_s^x a(\xi)\, d\xi \right) \tag{31}$$

Finally, the predicted final speed is derived from Eq. (30) as

$$\hat{V}(x_f) = \sqrt{\Phi(x_f; x)\{V(x)\}^2 + 2\int_x^{x_f} \Phi(x_f; s) b(s)\, ds} \tag{32}$$

Therefore, the proposed approximation scheme predicts the final speed by calculating scalar definite integrals instead of solving differential equations by using an explicit numerical integration method, e.g., forward Euler method. The coefficient functions $a(x)$, $b(x)$, and the state transition function $\Phi(x_f; s)$ are needed to evaluate the definite integrals. In the ideal case where the flight path remains fixed during flight, the associated functions and integrals do not need to be calculated again. Therefore, online evaluation of Eq. (32) can be performed without severe computational burden by simply reading out necessary quantities from the tables storing offline computation result. Otherwise, the coefficient functions and the state transition function entering into the definite integrals can be re-calculated for consistency with the online-updated output of the path generator. Computation of the definite integrals can be performed more efficiently than numerically propagating the dynamics, thus, the proposed method promotes online prediction as long as the approximation introduced in Eq. (27) is valid enough.

3.4 Desired Speed Targetting

A rough understanding about the flight physics is that flying at a relatively lower altitude leads to a smaller final speed since the drag increases with the atmosphere becoming dense at low altitude regime, and a more curved and longer path results in greater loss of energy as the induced drag increases when the vehicle performs more lateral manoeuvres. In this sense, the trajectory planning can be accomplished

by finding the shaping parameter R^* for fixed (p, h_{des}) such that

$$R^* = \arg\min_R \left| \hat{V}_f(R) - V_{f_d} \right| \tag{33}$$

where $\hat{V}_f(R)$ represents the estimated final speed $\hat{V}\left(x_f\right)$ that can be written conceptually as

$$\hat{V}_f(R) = \mathsf{speed\_predictor}\left(\mathsf{path\_generator}\left(R; p, h_{des}\right)\right) \tag{34}$$

with path_generator yielding an altitude profile and speed_predictor calculating the final speed by propagating the vehicle dynamics along the given path. The targetting process of Eq. (33) can be performed in each trajectory update cycle by leveraging a numerical procedure for root finding or line search, which requires iterations in its nature. This shows why a light speed prediction algorithm is advantageous for online execution. The result corresponding to R^* can be taken as the trajectory planning solution for a given instance. The planned trajectory can be used as a reference for trajectory tracking, or it can be used to compute the lift acceleration command at each instance as explained in Eq. (15).

4 Numerical Simulation

This section presents numerical simulation examples to demonstrate the proposed guidance algorithm. Table 1 summarises the simulation parameters including the initial conditions, the desired final conditions, and the vehicle dynamics model data. The models used for the atmospheric density and the drag coefficient are represented as

$$\rho(h) = \rho_0 \exp\left(-\frac{h}{H}\right) \tag{35}$$

$$C_D = C_{D_0} + K{C_L}^2 \tag{36}$$

where ρ_0 is the atmospheric density at the sea level, H is a constant scale factor, C_{D_0} is the zero-lift drag coefficient, and K is the induced drag coefficient. The model parameters are borrowed from [4]. At this stage, the present study does not consider uncertainties such as modelling inaccuracies or wind disturbances in the model parameters used for speed prediction. `Convex.jl` and `MOSEK` are used to model and to solve QP, respectively, in the process of path generation. The Brent's method is used to find R^* via line search in the process of desired speed targetting. Note that minimisation over a bounded interval is more robust than root finding to perform desired speed targetting. The simulation software is developed in Julia and is accessible via [8].

The following simulation shows i) the actual trajectory simulated with the true dynamics model using the lift acceleration command computed from the initial trajectory planning result according to Eq. (15) (sky blue line, PlanSim), ii) the actual trajectory simulated with the true dynamics model using the lift acceleration command that is updated periodically by repeating the trajectory planning process during flight (orange line, RePlanSim), and iii) the snapshot of the trajectory planning result obtained with the approximate prediction method once at the initial instance (green line, Plan).

Figure 1 shows the downrange histories for the trajectory variables including altitude, flight path angle, speed, and lift acceleration. Also, Fig. 2 shows the time histories for the same trajectory variables along with downrange, and planned trajectory parameters. Table 2 lists the achieved final values of V and γ for various update periods of online trajectory replanning Δt_{update} for RePlanSim. The figures and the table show that the proposed planning algorithm achieves the desired final position as well as the desired final velocity in terms of both the magnitude and the direction. Periodic update of the planned trajectory realises feedback by considering the current state as the initial condition for prediction performed at each update cycle, thus effectively closing the loop.

Table 1 Simulation Parameters

Quantity	Unit	Value	Quantity	Unit	Value
x_0	m	0	h_0	m	3,000
γ_0	deg	5	V_0	m/s	1,000
x_f	m	40,000	h_{f_d}	m	0
γ_{f_d}	deg	−30	V_{f_d}	m/s	400
p	–	10	n	–	1.5
m	kg	544	S	m^2	0.258
C_{D_0}	–	0.126	K	–	0.370
g	m/s^2	9.805	ρ_0	kg/m^3	1.225
H	m	8,435			

Table 2 Simulation Results: Final Velocity

Case	Plan	PlanSim	RePlanSim				
Δt_{update} [s]	-	-	1	2	5	10	20
$V(t_f)$ [m/s]	400.00	398.97	399.57	399.56	399.51	399.37	399.20
$\gamma(t_f)$ [deg]	−30.000	−29.994	−29.993	−29.994	−29.994	−30.000	−29.992

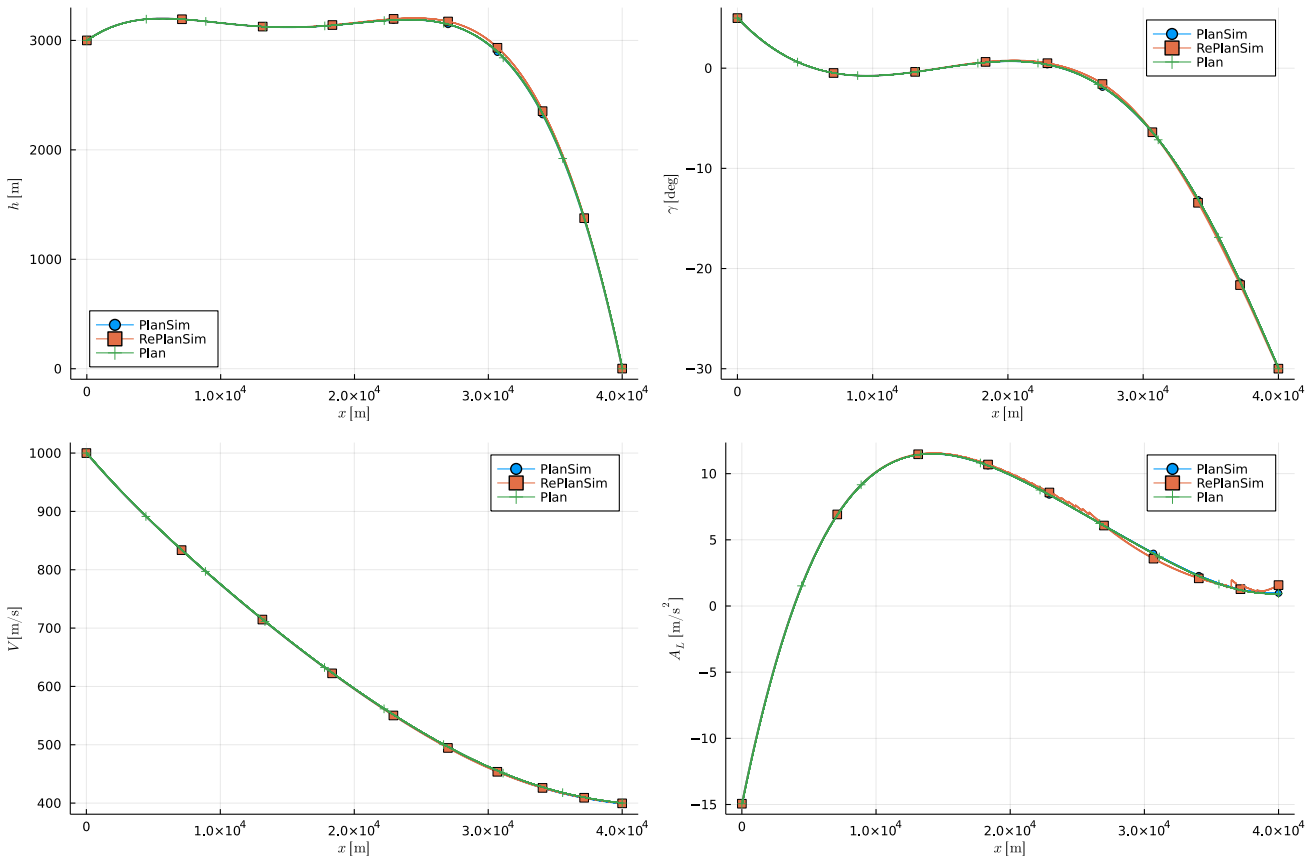

Fig. 1 x-Referenced Simulation Results

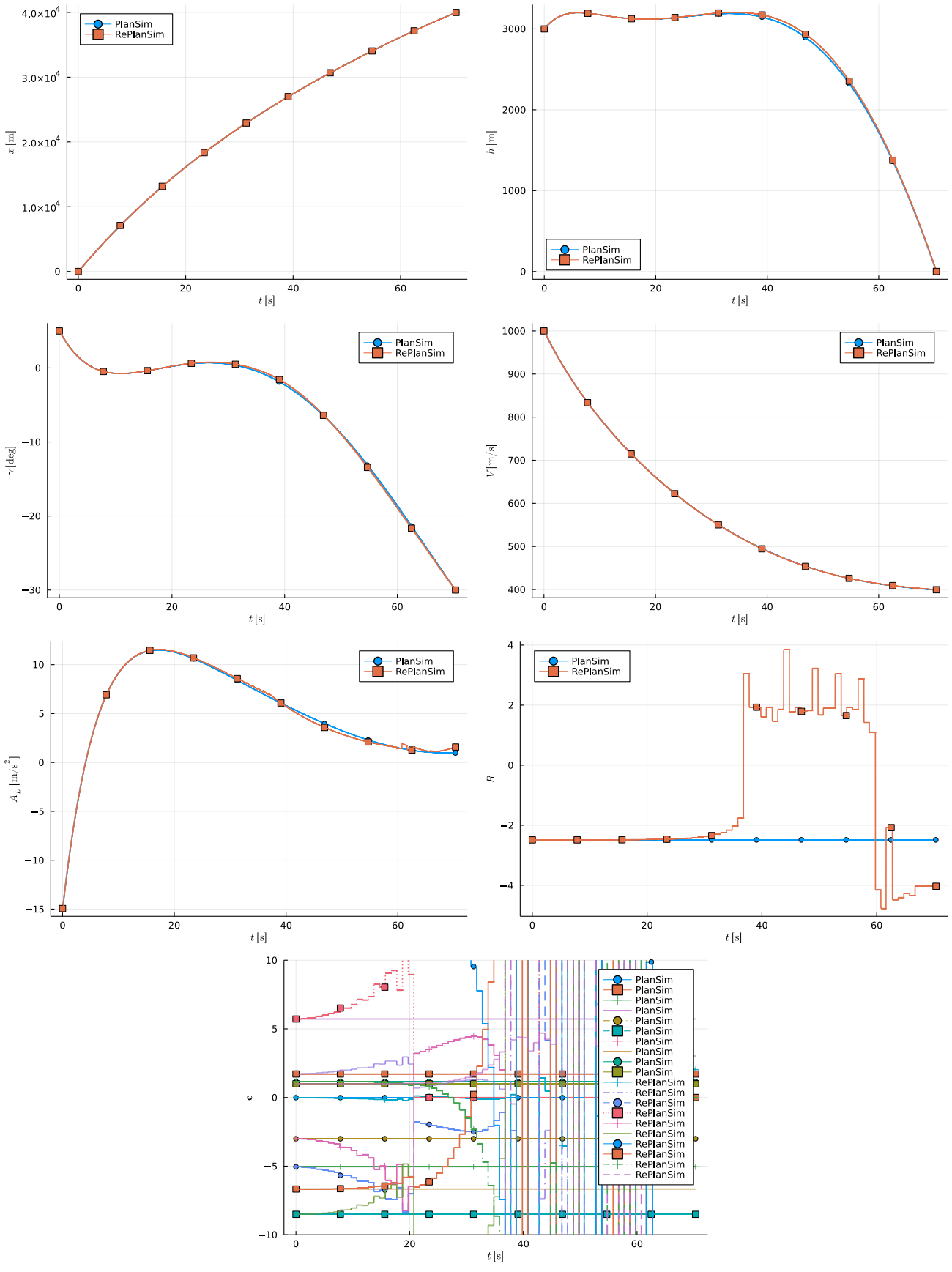

Fig. 2 t-Referenced Simulation Results

5 Conclusion

A guidance algorithm was developed for an unpowered endoatmospheric vehicle to achieve a desired speed at the final time in addition to satisfying the position and flight path angle boundary conditions. Unlike the guidance problems that can be fully resolved by considering only the kinematics of motion, the energy dissipation requirement adds considerable complexity to the design of a low-latency feedback guidance algorithm based on the predictive control principle. This is mainly due to the lack of a simple analytical solution for the dynamics of the vehicle speed which is model-dependent and underactuated. To address this difficulty, this study developed a guidance algorithm that performs iterative targetting of the desired final speed by using an approximate speed prediction method that brings improvements in computational efficiency over the brute-force numerical propagation through the semi-analytical solution for the speed. Along with the path generator producing altitude profiles based on convex optimisation, the overall composition of the proposed algorithm was sought to reduce the amount of online computation so that it suits well with the purpose of online trajectory update. The effectiveness of the proposed algorithm for energy management trajectory planning was demonstrated via numerical simulation. As the directions for further research, one may pursue developing an advanced algorithm that considers the effects of environmental perturbation such as wind, and combining the proposed guidance algorithm with a model learning technique for estimating the uncertain aerodynamic data will enable more robust trajectory planning.

References

[1] H. L. Ehlers and J. W. Kraemer. Shuttle orbiter guidance system for the terminal flight phase. *Automatica*, 13(1):11–21, 1977. DOI: 10.1016/0005-1098(77)90005-X.

[2] Jon C. Harpold and Donald E. Gavert. Space shuttle entry guidance performance results. *Journal of Guidance, Control, and Dynamics*, 6(6):442–447, 1983. DOI: 10.2514/3.8523.

[3] Kenneth D. Mease and Jean-Paul Kremer. Shuttle entry guidance revisited using nonlinear geometric methods. *Journal of Guidance, Control, and Dynamics*, 17(6):1350–1356, 1994. DOI: 10.2514/3.21355.

[4] Min-Jea Tahk, Gun-Hee Moon, and Sang-Wook Shim. Augmented polynomial guidance with terminal speed constraints for unpowered aerial vehicles. *International Journal of Aeronautical and Space Sciences*, 20:183–194, 2019. DOI: 10.1007/s42405-018-0093-4.

[5] Gun-Hee Moon, Min-Jea Tahk, Du Hee Han, and JaeYeol Son. Generalized polynomial guidance for terminal velocity control of tactical ballistic missiles. *International Journal of Aeronautical and Space Sciences*, 22:163–175, 2021. DOI: 10.1007/s42405-020-00291-6.

[6] Youngil Kim, Namhoon Cho, Jongho Park, and Youdan Kim. Design framework for optimizing waypoints of vehicle trajectory considering terminal velocity and impact angle constraints. *Engineering Optimization*, Online Published, 2021. DOI: 10.1080/0305215X.2021.1925264.

[7] Young-Sam Kim and Min-Jea Tahk. Auto-landing guidance for unmanned aerial vehicle with engine flameout. *Proceedings of the Institution of Mechanical Engineers, Part G: Journal of Aerospace Engineering*, 233(13):4864–4878, 2019. DOI: 10.1177/0954410019831501.

[8] Namhoon Cho. FlightGNC.jl. https://github.com/nhcho91/FlightGNC.jl, October 2021.